0026-895X/04/6506-1517–1525$20.00
MOLECULAR PHARMACOLOGY
Copyright © 2004 The American Society for Pharmacology and Experimental Therapeutics
Mol Pharmacol 65:1517–1525, 2004

Vol. 65, No. 6
3134/1153869
Printed in U.S.A.

Alternative Processing Events in Human *FMO* Genes

Virginie Lattard, Jun Zhang, and John R. Cashman

Human BioMolecular Research Institute, San Diego, California

Received December 2, 2003; accepted March 9, 2004

This article is available online at http://molpharm.aspetjournals.org

ABSTRACT

In humans, flavin-containing monooxygenase (FMO) functional diversity is determined by the expression of five *FMO* genes, named *FMO1* to *FMO5,* and their variants. In this study, we systematically analyzed transcripts of *FMO1* to *FMO5* in different human tissues by reverse-transcription-polymerase chain reaction and identified a large number of splice variants. Exon skipping was the major splicing event observed. Normally spliced transcripts were generally the prominent transcript detected. For *FMO1*, *FMO2*, and *FMO3*, two to three different splice variants were identified, and their corresponding expression was always low in the tissues examined. For *FMO5* and particularly for *FMO4*, more complex alternative splice patterns were observed, with five and seven splice variants detected, respectively. Most identified FMO splice variants either caused a frame-shift or lacked essential functional sites. The corresponding transcripts were therefore incapable of encoding a functional enzyme and were not analyzed further in this study. However, a common in-frame exon 3- (exon 4 for FMO4) deleted variant, leading to the deletion of 63 amino acids, was identified for *FMO1*, *FMO3*, *FMO4*, and *FMO5*. To examine the functional importance of exon 3-deletion, FMO1, FMO3, FMO4 and the corresponding exon-deleted proteins were expressed as fusion proteins. Activity studies were done with two selective functional FMO substrates, methimazole, and 10-(*N*,*N*-dimethylaminopentyl)-2-(trifluoromethyl)phenothiazine and exon 3- (exon 4 for FMO4) deleted FMOs were not able to catalyze the *S*- and *N*-oxygenation of these substrates, respectively. It is not clear whether these FMO splice variants can oxygenate other substrates, including those that remain to be discovered.

The flavin-containing monoxygenases (FMOs) are a family of enzymes that catalyze the oxygenation of numerous nitrogen-, sulfur-, phosphorous-, and other nucleophilic heteroatom-containing chemicals, drugs, and xenobiotics (Ziegler, 1988; Cashman, 1995). Each FMO exhibits distinct substrate specificity. However, FMOs show overlapping substrate specificity among the family members. Current information indicates that FMO functional diversity is contributed by the expression of five human *FMO* genes, named *FMO1* to *-5* (Lawton et al., 1994; Hines et al., 2002), and their variants. A sixth *FMO* gene was described but apparently is a pseudogene (Hines et al., 2002). The six human *FMO*s are localized on chromosome 1q and exist in a single gene cluster, except for *FMO5* (Shephard et al., 1993; McCombie et al., 1996). The six human FMOs share 50 to 80% sequence identity (Lawton et al., 1994). All six *FMO*s contain eight coding exons. The boundaries and sizes of these coding exons are highly conserved among family members and across animal species. Expression of FMOs is tissue- and species-dependent (Hines et al., 1994). In tissues in which the amount of FMO is abundant, the apparent activity seems to be correlated with immunoreactivity and has been found to be dominated by the most prominent FMO expressed. For example, FMO3 is the most catalytically important isoform in adult human liver (Lomri et al., 1992), whereas in adult human kidney, FMO1 is the most prominent form (Dolphin et al., 1996). In tissues in which expression level of FMO is less abundant, such as in human brain, the dominant FMO functional activity is less clear and the characterization of prominent FMO activity in these tissues has been challenging.

Besides gene duplication and divergence, alternative splicing of the primary RNA transcript is another mechanism for generating protein diversity for gene families. With the completion of the human genome sequence, it has become apparent that alternative splicing probably contributes to the complexity of the proteome much more than previously recognized (Mironov et al., 1999). Alternative splicing has been characterized for a number of cytochrome P450 genes. Alternative splicing, through mechanisms of alternating exons, exon skipping, exon scrambling, and alternating splicing sites, has led to the expression of novel cytochrome P450 isoforms with unique catalytic activity and substrate specificity (Zaphiropoulos, 1996; Christmas et al., 2001; Domanski et al., 2001). Information describing alternative RNA processing for human *FMOs* is available only for the human

This work was supported by National Institutes of Health grant DK59618.
V.L. and J.Z. contributed equally to this article.

ABBREVIATIONS: FMO, flavin-containing monooxygenase; PCR, polymerase chain reaction; RT, reverse transcriptase; bp, base pair(s); MBP, maltose-binding protein; 5-DPT, 10-(*N*,*N*-dimethylaminopentyl)-2-(trifluoromethyl)phenothiazine; PAGE, polyacrylamide gel electrophoresis.

FMO6 gene (Hines et al., 2002). Examination of *FMO6* transcripts amplified from human liver RNA showed skipping of exons and/or using of alternative splice sites in introns. None of the transcripts detected for human *FMO6* were full length; thus, *FMO6* transcripts are rendered incapable of encoding a functional FMO6 enzyme. Therefore, human *FMO6* is predicted to be a pseudogene. In other animals, there are also limited reports of FMO alternative splicing events. Rabbit *FMO1* has been shown to have two upstream noncoding exons and to exhibit tissue-specific alternative splicing (Luo and Hines, 1996, 1997). An alternative transcript of rat *FMO4* has been identified in rat brain as a result of exon 4 skipping (Lattard et al., 2003). With the skipping of exon 4 (i.e., a 189-bp fragment), the alternative transcript retains the reading frame and encodes a protein still containing the NADPH- and FAD-binding sites. Such an FMO4 without exon 4 could still have functional activity. Even if tissue-specific expression profiles of FMOs are quite distinct between animal species, information regarding alternative splicing in animals could still help resolve possible variations in humans. To further our understanding of the expression profile of human FMO1 to FMO5, we systematically studied the transcripts of *FMO1* to *FMO5* in multiple human tissues. With the focus on FMO coding exons, our goal was to characterize the prominent alternative splicing events for FMOs in different human tissues at different points in development and identify potentially novel functional FMO isoforms.

Materials and Methods

Chemicals. DNA polymerases and cDNA synthesis components were purchased from Invitrogen (Carlsbad, CA) and Promega (Madison, WI). All chemicals and reagents were purchased from Aldrich Chemical Co. (Milwaukee, WI) in the highest purity commercially available. The components of the NADPH generating system were obtained from Sigma Aldrich (St. Louis, MO). Buffer and other agents were purchased from VWR Scientific, Inc., (San Diego, CA). The phenothiazine analog 10-(*N*,*N*-dimethylaminopentyl)-2-(trifluoromethyl)phenothiazine (5-DPT) was synthesized by the method described previously (Brunelle et al., 1997).

Total Tissue Samples. The ethics committee of Independent Review Consulting Inc. (San Anselmo, CA) approved this study. Tissue samples were obtained from the Brain and Tissue Bank for Development and Disorder at the University of Miami (Miami, FL), the Brain and Tissue Bank for Developmental Disorders at the University of Maryland (Baltimore, MD), and Stanford Research International (Menlo Park, CA). Total RNA was extracted from adult human brains and livers using TRIzol reagent (Invitrogen). Adult human liver total RNA was isolated from normal livers pooled from a total of 10 male/female white persons (aged 17 to 59 years). Human adult brain total RNA was isolated from normal brains pooled from 10 male/female white persons (aged 14 to 56 years). Total RNA concentrations were evaluated spectrophotometrically with UV absorbance at 260 nm.

Human fetal liver, human fetal brain, and human kidney total RNA were purchased from BD Biosciences Clontech Inc., (Palo Alto, CA). Based on information provided by the vendor, total RNA of corresponding tissues was isolated from human fetal livers pooled from a total of 63 spontaneously aborted male/female white fetuses (22–40 weeks), from human fetal brains pooled from a total of 24 spontaneously aborted male/female white fetuses (16–32 weeks), and from normal human kidneys pooled from a total of six male/female white persons (aged 28 to 52 years).

Reverse Transcriptions. Five different first-strand cDNAs were synthesized in the presence of five specific reverse primers RT1, RT2, RT3, RT4, and RT5 (Table 1) designed from human *FMO1* (GenBank accession number 4503754), *FMO2* (GenBank accession number 4503756), *FMO3* (GenBank accession number 31542790), *FMO4* (GenBank accession number 4503758), and *FMO5* (GenBank accession number 4503760) cDNA sequences, respectively. First-strand cDNA templates were synthesized from 1 μg of total RNA from adult human kidney, liver, and brain and from fetal human liver and brain in the presence of specific primers (50 pmol) in 20 μl of standard reverse transcription buffer (20 mM Tris-HCl, pH 8.4, 5 mM $MgCl_2$, 50 mM KCl, and 10 mM dithiothreitol) and 500 μM of each deoxynucleotide triphosphate. After an initial denaturation step at 65°C for 5 min, Superscript II reverse-transcriptase (50 U, Invitrogen) was added and the reaction was incubated for 50 min at 42°C and then for 15 min at 70°C.

Direct-PCR Amplifications. One microliter of FMO cDNAs resulting from reverse transcriptions was amplified by PCR using specific primers designed from human FMO1, -2, -3, -4, and -5 cDNAs and genomic DNAs. Primers were specifically designed from individual exons (Table 2). Different combinations of primers were used to examine different overlapping regions of the cDNA (from exon 1 or 2 to 5, from exon 3 to 7, from exon 5 or 6 to 9, from exon 2 or 3 to 9, and, only for FMO4, from exon 4 to 8). PCR was done using different combinations of primers (20 pmol), 1 unit of *Taq* DNA polymerase (Promega) in a total volume of 50 μl of 1.5 mM $MgCl_2$ PCR buffer (10 mM Tris-HCl, pH 9.0, 50 mM KCl, and 0.1% Triton-X100) and 200 μM of each deoxynucleotide triphosphate. Amplifications were done at 94°C for 3 min, 35 cycles of 94°C for 30 s, 60°C for 30 s, and 72°C for 1 min, followed by a final extension at 72°C for 5 min. Amplification products were fractionated by electrophoresis on 1% agarose gel and visualized by ethidium bromide staining. The different PCR-products were gel-purified (QIAquick gel-extraction kit; QIAGEN, Valencia, CA) and sequenced in both directions (Allele Biopharmaceutical Inc., San Diego, CA).

Nested PCR Amplifications. First-step PCR-amplifications were done as described above, using specific forward and reverse primers designed from exons 1 and 9 (or 10 for FMO4), respectively, of the human FMO1, -2, -3, -4, and -5 cDNAs (Table 2). Amplifications were done at 94°C for 3 min, 25 cycles of 94°C for 30 s, 60°C for 30 s and 72°C for 2 min, followed by a final extension at 72°C for 5 min.

PCR products were further re-amplified by PCR using the same combination of primers as those used for the direct PCR-amplifications described above (from exon 1 or 2 to 5, from exon 3 to 7, from exon 5 or 6 to 9, from exon 2 or 3 to 9, and only for FMO4 from exon 4 to 8). Amplifications were done at 94°C for 3 min, 35 cycles of 94°C for 30 s, 60°C for 30 s, and 72°C for 1 min, followed by a final extension at 72°C for 5 min. PCR-products were fractionated by electrophoresis on 1% agarose gel and visualized. PCR-products were gel-purified and sequenced in both directions.

Amplifications of Exon 3 (Equivalent to Exon 4 for FMO4)-Skipped Variants for FMO1 to FMO5. Forward splice variant primers SP1 to SP5 were specifically designed to amplify exon 3 splice variants (Table 3) for FMO1 to FMO5, respectively. The specific splice variant primers were composed of 16 to 19 terminal nucleotides of exon 2 (equivalent to exon 3 for FMO4) and 2 to 4 initial nucleotides of exon 4 (equivalent to exon 5 for FMO4) (Table 3). From the PCR-products obtained for the first PCR-amplification

TABLE 1
Reverse transcription primers of FMO1, FMO2, FMO3, FMO4, and FMO5

Primer	Target	Exon	Sequence
RT1	FMO1	9	ccttcccatttcctg
RT2	FMO2	9	tttgtttctgggtgaagatg
RT3	FMO3	9	cacaaggaaaacagcg
RT4	FMO4	10	agcagttatgatggagagcag
RT5	FMO5	9	gcgattttataccgatgctg

described above, a re-amplification was done in the presence of the forward splice variant primer SP1, SP2, SP3, SP4, or SP5 (20 pmol) and the corresponding reverse primers belonging to exon 9 (exon 7 and 10 for FMO4). Amplifications were done at 94°C for 3 min, 35 cycles of 94°C for 30 s, 61°C for 30 s and 72°C for 1 min, followed by a final extension at 72°C for 5 min. PCR-products were fractionated by electrophoresis on 1% agarose gel and visualized. PCR-products were gel-purified and sequenced in both directions.

Wild-type FMO1, -2, -3, -4, or -5 plasmids and corresponding exon 3- (equivalent to exon 4 for FMO4) deleted plasmids were used as negative and positive controls, respectively.

Cloning, Expression, and Purification of N-Terminal Maltose Binding Protein, C-Terminal Poly-Histidine Fusion Wild-Type and Exon 3- or 4-Deleted FMOs. Wild-type human FMO1, FMO3, and FMO4 and the corresponding exon 3- or 4-deleted variants, respectively, were expressed as N-terminal maltose-binding protein (MBP) C-terminal poly-histidine (His_6) fusion proteins. Wild-type FMO1, FMO3, and FMO4 were amplified from fetal or adult liver and kidney, respectively, using specific primers designed from the corresponding cDNA sequences (GenBank accession numbers 4503754, 31542790, 4503758, respectively). The reverse primers used for amplification included an 18-nucleotide sequence encoding six histidines, allowing addition of a histidine tag to the cDNAs. Wild-type FMO1-His_6, FMO3-His_6, and FMO4-His_6 were subcloned into the expression vector pMAL-c2 and used as templates to construct the corresponding exon 3- or 4-deleted variants (i.e., MBP-FMO1-Δex3-His_6, MBP-FMO3-Δex3-His_6, MBP-FMO4-Δex4-His_6)

Escherichia coli JM109 cells were transformed with MBP-FMO1-His_6, MBP-FMO1Δex3-His_6, MBP-FMO3-His_6, MBP-FMO3-Δex3-His_6, MBP-FMO4-His_6, or MBP-FMO4-Δex4-His_6 plasmid and grown at 37°C in modified Hanahan's broth medium (2% bactotryptone, 0.5% yeast extract, 8 mM NaCl, 10 mM $MgCl_2$, 2.5 mM KCl, and 20 mM glucose) to a UV absorbance of 0.5 to 0.6 at 600 nm. Isopropyl-β-thio-galactopyranoside (0.2 mM), riboflavin (0.05 mM), and 100 μg/ml ampicillin were then added. The cells were incubated overnight with constant shaking at 30°C. Cells were harvested by centrifugation at 6000*g* for 10 min and re-suspended in lysis buffer (20 mM phosphate, pH 7.4, 200 mM NaCl, and 0.5% Triton X-100) containing 0.2% L-α-phosphatidylcholine and 0.5 mM phenylmethylsulfonyl fluoride. After incubation for 30 min at 4°C, the re-suspended cells were disrupted by sonication (i.e., 30-s bursts separated by periods of cooling), then centrifuged at 18,000*g* for 30 min at 4°C. The resulting supernatant was purified with an amylose column (New England Biolabs, Beverly, MA) as described previously (Brunelle et al., 1997). The amylose-affinity column eluate was then applied to a HisTrap Chelating column (HisTrap Kit; Amersham Biosciences, Piscataway, NJ) equilibrated with buffer A (20 mM phosphate, pH 7.4, 0.5 M NaCl, 10 mM imidazole, and 0.5% Triton X-100) according to the manufacturers' specifications. After washing with buffer A, bound proteins were eluted with 200 mM imidazole in buffer A. Eluted fractions were fractionated by SDS-PAGE (Laemmli, 1970) and visualized by Coomassie blue staining.

The viability of wild-type proteins and corresponding variants was investigated by examining the oxygenation of specific FMO-substrates. Methimazole *S*-oxygenation was determined according to the method of Dixit and Roche (1984). The *N*-oxygenation of 5-DPT was determined as described previously (Brunelle et al., 1997).

TABLE 2
Primers used for direct or nested FMO PCR amplification
The primers used for the first PCR amplification during nested PCR are in bold.

Target and Exons	Forward/Reverse	Sequence
FMO1		
1	Forward	**tgctaataccagagtcctgcgtgg**
3	Forward	gtctctacaagtctgtggtttccaacag
5	Reverse	gtgccagaatttcccattccaatc
5	Forward	gcacagacattgctgtggaggc
7	Reverse	ctttcccagtgatgcgtcc
9	Reverse	**gagaacaggttgggttttgcattg**
FMO2		
1	Forward	**ccaagggagaaaactattct**
2	Forward	atggcaaagaaggtagctgtg
3	Forward	tggaagatggccgagcaagta
5	Reverse	ggcggctatggaaatattgg
6	Forward	tgccacgaacagctgtaaaatg
7	Reverse	caccttgatggctccacaga
9	Reverse	**tttgtttctgggtgaagatg**
FMO3		
1	Forward	**gttggacaggacgtagacacacagaag**
2	Forward	ccatcattggagctggtgtgag
3	Forward	ccaactttatgcacaacagcaagatc
5	Reverse	gttctttatagtccctgctgtggaagc
5	Forward	tgccacagaactcagccgca
7	Reverse	cgttaaatacaggctctttcctcagg
9	Reverse	**ttgccccaatgaaggaggagag**
FMO4		
1	Forward	**gagggcacttttacaaaagtcatctttc**
2	Forward	gaagctgtctaaacctcctactc
3	Forward	ggagctggtgtgagtggcctct
4	Forward	ctatctccaagaatttgctgagcactt
5	Reverse	tctctgtgacaacatcccactgacc
6	Forward	gctgtggaactcagtcgaacgg
7	Reverse	ggatagccccaatctgaagagcg
8	Reverse	ccccacagaggatacagtttggc
10	Reverse	**gtgcctatgcaggcagcgata**
FMO5		
1	Forward	**ccagatcgcagctgaaggat**
2	Forward	atgactaagaaaagaattgctgtg
3	Forward	tcatgcataatgcccaggtc
5	Reverse	tgtggaagtactgccctttgaactt
6	Forward	atatggaagatctgtggccaatca
7	Reverse	ttcactttcaccaagccagaaa
9	Reverse	cccaccaaatcagcaagctc
9	Reverse	**gcgattttataccgatgctg**

Results

To systematically characterize transcripts of *FMO1* to *FMO5* from human tissues, we designed specific primers in different exons to analyze overlapping regions of the cDNA through RT-PCR analysis. To minimize nonspecific amplifications, gene-specific anti-sense primers (RT1–5; Table 1) were used to generate the first strand cDNAs from FMO1 to FMO5 used in subsequent PCR studies. Direct PCR amplification allowed the comparison of the expression levels of FMO1 to FMO5 in different tissues (A in Figs. 1, 3, 4, and 5). Nested PCR amplification allowed the specific identification of alternatively spliced FMO transcript variants from different tissues (B in Figs. 1–5). Nested PCR-amplification of FMO1 to FMO5 from human tissues showed multiple alternative splicing variants. Because nested PCR-amplification was a very sensitive method and could possibly amplify non-specific or low-frequency error products, only PCR-products reproducibly observed were considered. Certain alternative splicing products were detected through direct PCR, but not through nested PCR, because of preferential competitive am-

TABLE 3
Forward splice variant primers SP1 to SP5 designed specifically to amplify exon 3 (equivalent to exon 4 for FMO4)-deleted FMO variants
Nucleotides belonging to exon 4 (equivalent to exon 5 for FMO4) are indicated in bold.

Primers	Target	Exon	Sequence
SP1	FMO1	2/4	gctgtggagattcacc**ac**
SP2	FMO2	2/4	gagtgtggaggttcaaa**ac**
SP3	FMO3	2/4	cctgtggaaattttca**aca**
SP4	FMO4	3/5	gggattatggaagtttact**acca**
SP5	FMO5	2/4	gctctggaggttccag**ac**

plification of other PCR products in the same reaction. Therefore, the intensity of the bands obtained after nested PCR did not reflect the relative level of each splice variant. All splice variants indicated specifically in each figure have been fully sequenced to verify the alternative splicing events.

Splice Variants of FMO1. The expression level of FMO1 mRNA was examined by direct PCR amplification in different tissues (i.e., pools of kidneys, livers, and brains) obtained from fetal or adult human samples (Fig. 1A). For all the overlapping regions examined, normally spliced FMO1 transcripts were readily detected in kidney (lane 1), fetal liver (lane 2), and fetal brain (lane 4). No other transcript was observed after direct PCR-amplification. From adult liver (lane 3) and adult brain (lane 5), FMO1 mRNA was nondetectable after only direct PCR-amplification (Fig. 1A). Only after the amplification was done from exons 5 to exon 9 were faint signals corresponding to normally spliced FMO1 observed in adult liver and adult brain.

The presence of putative FMO1 splice variants was studied by using nested PCR-amplifications. Different overlapping regions of the FMO1 cDNA were examined. These amplifications were repeated three times and a representative gel was shown (Fig. 1B). Expression of the normally spliced FMO1

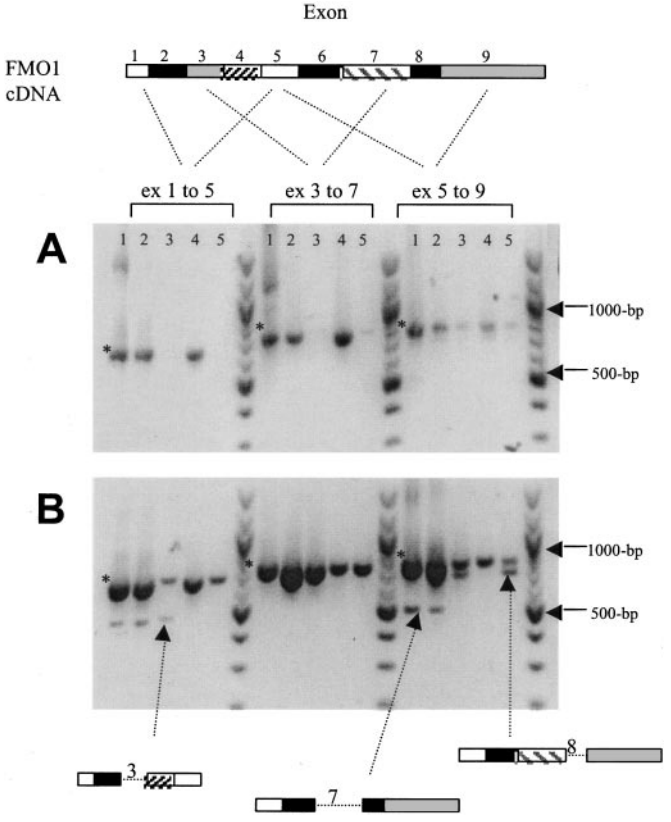

Fig. 1. Alternative processing of the human FMO1 transcript shown by RT-PCR amplification. A diagram of human FMO1 cDNA is shown at the top (each exon is illustrated with different patterned boxes). Specific FMO1 cDNA was synthesized, as described under *Materials and Methods*, from 1 μg of RNA from adult human kidney (lane 1), fetal human liver (lane 2), adult human liver (lane 3), fetal human brain (lane 4), and adult human brain (lane 5). Overlapping fragments (i.e., exons 1–5, 3–7, and 5–9) were amplified with direct PCR (A) or nested PCR (B). The normally spliced transcript is shown with an asterisk. Alternative splice variants are indicated by arrows and illustrated according to the sequence analysis (blocks represent existing exons and dotted lines represent skipping exons).

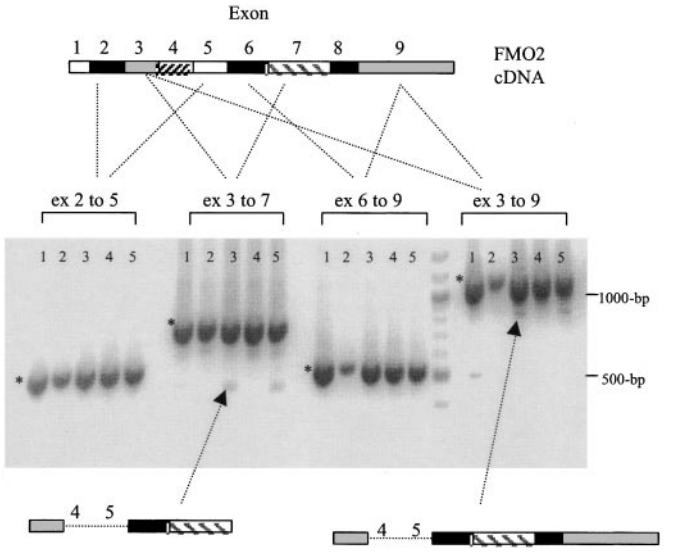

Fig. 2. Alternative processing of the human FMO2 transcript shown by RT-PCR amplification. A diagram of human FMO2 cDNA is shown at the top (each exon is illustrated with different patterned boxes). Specific FMO2 cDNA was synthesized, as described under *Materials and Methods*, from 1 μg of RNA from adult human kidney (lane 1), fetal human liver (lane 2), adult human liver (lane 3), fetal human brain (lane 4), and adult human brain (lane 5). Overlapping fragments (i.e., exons 2–5, 3–7, 6–9, and 3–9) were amplified with nested PCR. The normally spliced transcript is shown with an asterisk. Alternative splice variants are indicated by arrows and illustrated according to the sequence analysis (blocks represent existing exons and dotted lines represent skipping exons).

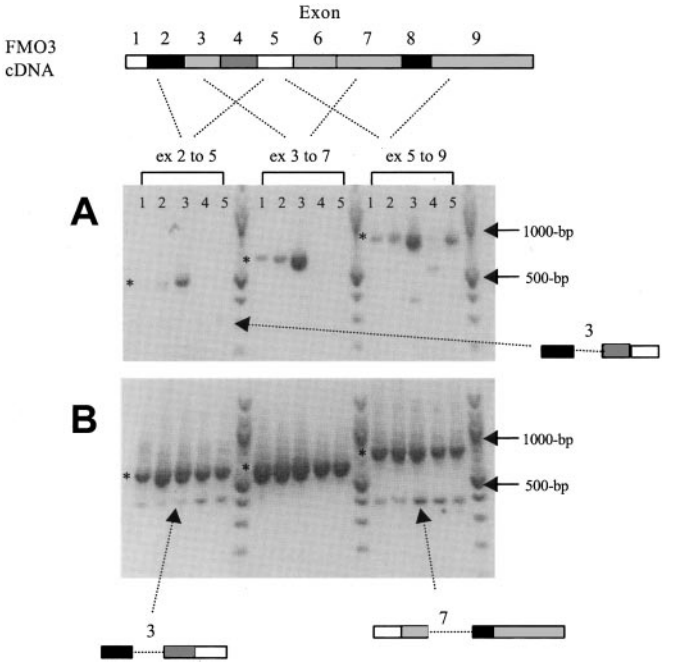

Fig. 3. Alternative processing of the human FMO3 transcript shown by RT-PCR amplification. A diagram of human FMO3 cDNA is shown at the top (each exon is illustrated with different patterned boxes). Specific FMO3 cDNA was synthesized, as described under *Materials and Methods*, from 1 μg of RNA from adult human kidney (lane 1), fetal human liver (lane 2), adult human liver (lane 3), fetal human brain (lane 4), and adult human brain (lane 5). Overlapping fragments (i.e., exons 2–5, 3–7, and 5–9) were amplified with direct PCR (A) or nested PCR (B). The normally spliced transcript is shown with a star. Alternative splice variants are indicated by arrows and illustrated according to the sequence analysis (blocks represent existing exons and dotted lines represent skipping exons).

was predominant in all the tissues examined (Fig. 1B). Only three alternative splice variants were reproducibly identified (Table 4): skipping of exon 3 (i.e., a 189-bp fragment) was observed from all tissues, skipping of a part of exon 7 (i.e., from nucleotide 916 of the cDNA sequence to the end of exon 7, a 268-bp fragment) was observed from kidney and fetal liver and skipping of exon 8 (i.e., a 73-bp fragment) was observed from adult liver, adult brain, and fetal brain (data not shown). Although skipping of exon 7 or 8 led to a frameshift, skipping of exon 3 did not modify the reading frame.

Splice Variants of FMO2. Direct PCR amplification from cDNA did not reveal detectable amplification products (data not shown). After nested PCR-amplification, the normally spliced FMO2 was the predominant form in all tissues examined (Fig. 2). Only a low level of alternatively spliced FMO2 forms were observed in the tissues examined. Nevertheless, two alternatively spliced products were reproducibly identified from various amplifications, one form with skipping of exon 4 + 5 (i.e., a 306-bp fragment) (Fig. 2) and the other form with skipping of exon 2 (i.e., a 138-bp fragment) (Table 4).

Splice Variants of FMO3. After direct PCR amplification (Fig. 3A), for all the overlapping regions examined, normally spliced FMO3 mRNA was strongly detected in adult liver (lane 3), faintly detected in adult kidney (lane 1) and fetal liver (lane 2) from human. In adult and fetal human brain, the FMO3 transcript was nondetectable except for the exon 5 to 9 amplification.

Nested PCR amplification studies (Fig. 3B) allowed the reproducible identification of only two splice variants: skipping of exon 3 (i.e., a 189-bp fragment) conserving the reading frame and skipping of exon 7 (i.e., a 356-bp fragment) leading to a frameshift (Table 4). Both splice variants were detected in all tissues. FMO3 splice variants were faintly detected only after direct PCR amplification (Fig. 3A) in human brain tissues. However, normally spliced FMO3 expression was always predominant in all the human tissues analyzed (i.e., brain, kidney, and liver).

Splice Variants of FMO4. The picture for splice variants of FMO4 was the most complex one observed among all the FMO members examined. After direct PCR amplification, FMO4 mRNA was detected in all tissues examined (Fig. 4A). FMO4 was readily detected from kidney and liver (lanes 1–3), and only faintly detected from brain (lanes 4–5). In contrast to other FMOs examined, normally spliced FMO4 was not always the predominant form detected. In kidney (lane 1) and liver (lanes 2–3), normally spliced FMO4 seemed to be the most prominent FMO4 form expressed. In brain (lanes 4–5), splice variants were more readily detectable than normally spliced FMO4, when particular fragments were amplified (i.e., from exons 2 to 5, from exons 4 to 8, from exons 6 to 10). Amplification from exon 2 to 5 allowed, in human brain only, the detection of an exon 4-skipped variant (i.e., a 189-bp fragment). Amplification from exons 4 to 8 allowed the identification of two kinds of alternative splicing: skipping of exon 7 (i.e., a 200-bp fragment) and skipping of exons 6 and 7 (i.e., a 343-bp fragment) in all tissues examined (Fig. 4A). In brain, both of these variants apparently were expressed at the same level as normally spliced FMO4. FMO4 amplification from exons 6 to 10 allowed the identification of an exon 8- and 9-skipped variant (i.e., a 423-bp fragment). Except for the exon 4- and exon 8- and 9-skipped variant, all these FMO4 deletions led to a frameshift (Table 4).

Nested PCR amplification studies (Fig. 4B) confirmed that significant expression of the splice variants identified above occurred and allowed the identification of three new splice variants that were nondetectable after only direct PCR-amplification: skipping of exons 3 + 4 (i.e., a 329-bp fragment) detected by the amplification from exons 1 to 5, skipping of

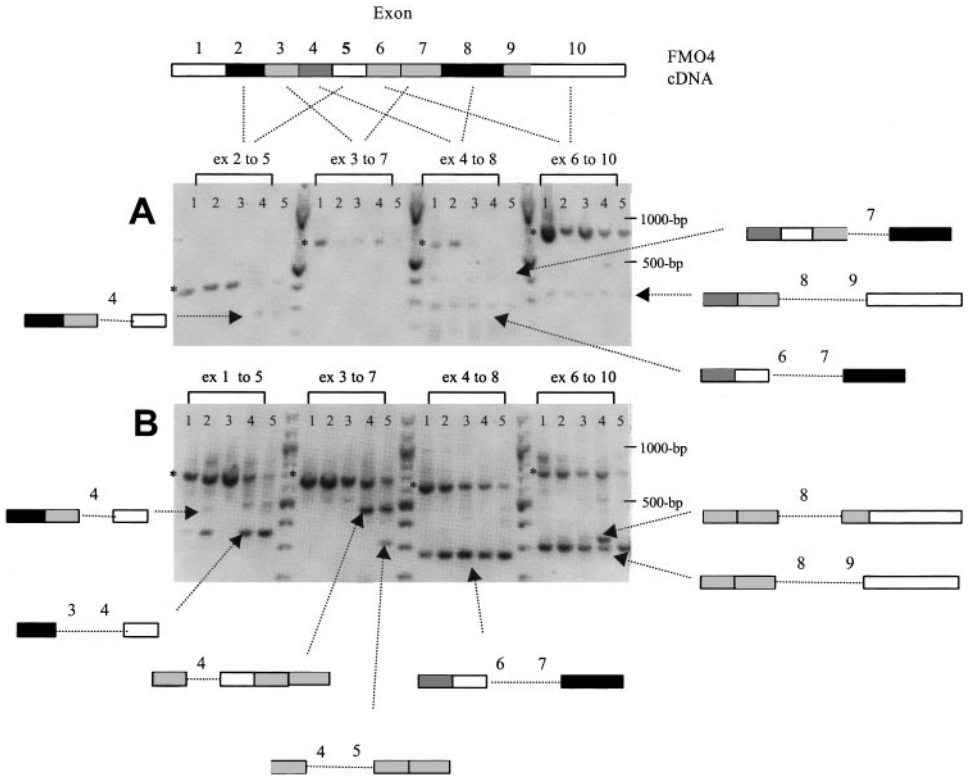

Fig. 4. Alternative processing of the human FMO4 transcript shown by RT-PCR amplification. A diagram of human FMO4 cDNA is shown at the top (each exon is illustrated with different patterned boxes). Specific FMO4 cDNA was synthesized, as described under *Materials and Methods*, from 1 μg of RNA from adult human kidney (lane 1), fetal human liver (lane 2), adult human liver (lane 3), fetal human brain (lane 4), and adult human brain (lane 5). Overlapping fragments (i.e., exons 1 or 2–5, 3–7, 4–8, and 6–10) were amplified with direct PCR (A) or nested PCR (B). The normally spliced transcript is shown with an asterisk. Alternative splice variants are indicated by arrows and illustrated according to the sequence analysis (blocks represent existing exons and dotted lines represent skipping exons).

exons 4 + 5 (i.e., a 352-bp fragment) detected by the amplification from exons 3 to 7 and skipping of exon 8 (i.e., a 353-bp fragment) detected by the amplification of exons 6 to 10, all of which led to a frameshift. These three splice variants were less prevalent than the normally spliced FMO4 transcript because they were not detectable after direct PCR-amplification (Fig. 4A).

Splice Variants of FMO5. The FMO5 transcript was readily detectable with a direct PCR-amplification from adult kidney, fetal liver, and adult liver (Fig. 5A, lanes 1–3) from human. From either fetal or adult brain, FMO5 transcripts were nondetectable with direct PCR. For all the FMO5 overlapping PCR-amplified regions examined, the normally spliced FMO5 was the predominant form detected. PCR fragments corresponding to skipping of exon 7 and skipping of exon 6 were only faintly detectable from kidney, fetal liver, and adult liver (Fig. 5A)

Nested PCR amplification studies of FMO5 transcripts from human kidney, liver, and brain samples revealed predominantly the normally spliced FMO5 form and also a number of poorly expressed alternative splice variants, including skipping of exon 3 (i.e., a 189-bp fragment), skipping of exon 6 (i.e., a 200-bp fragment), and skipping of exon 7 (i.e., a 353-bp fragment). These FMO5 alternative splice variants were detected in all tissues examined. In addition, FMO5 transcripts with skipping of exons 3–5 (i.e., a 495-bp fragment) and skipping of exons 6 and 7 (i.e., a 553-bp fragment) (data not shown) were also reproducibly observed.

Exon 3 (or Exon 4 for FMO4)-Skipped Variants in FMO1, -2, -3, -4, and -5. A nested PCR method was developed to specifically detect the exon 3 (or exon 4 for FMO4)-spliced forms of FMO (Fig. 6). For each FMO isoform, a forward primer was designed based on the junction between exon 2 and 4 (exons 3 and 5 for FMO4) and included the last 16 to 19 nucleotides of exon 2 (exon 3 for FMO4) and the first 2 to 4 nucleotides of exon 4 (Table 3). Reverse primers in exon 9 were used for FMO1, -2, -3, and -5 amplifications. Reverse primers in exons 7 and 10 were used for FMO4 amplification. PCR conditions were validated using wild-type FMO1, -2, -3, -4, or -5 plasmids and the corresponding exon 3 (or exon 4 for FMO4)-deleted plasmids to avoid nonspecific annealing with normally spliced transcripts.

For FMO1, exon 3-skipped transcripts were detected from all tissues (Fig. 6A). The FMO1 transcript with only exon 3 skipping was detected in kidney (lane 1), fetal and adult liver (lanes 2, 3), and fetal brain (lane 4) from human. The FMO1 exon 3-deleted transcript was not observed in adult human brain (lane 5). In brain and adult liver, exon 3 skipping was also observed associated with skipping of exon 7 or exons 7 and 8. For FMO2, no skipping of exon 3 was detected (Fig. 6B). For FMO3, skipping of exon 3 was observed in human kidney, liver, and fetal brain, with or without skipping of exon 7 (Fig. 6C). For FMO4, skipping of exon 4 was observed in all tissues. When exon 7 reverse primer was used to amplify exon 4-deleted FMO4 transcripts, single PCR products were observed in all tissues, indicating that skipping of exon 3 was not associated with skipping of exon 4, 5, or 6 in the presence of exon 7. However, when exon 10 reverse primer was used to amplify exon 4-deleted FMO4 transcripts, multiple PCR products were obtained. Sequencing analysis of the corresponding PCR products confirmed the presence of FMO4 transcripts with skipping of exon 3 in association with skipping of exon 9 and/or 8 and FMO4 transcripts with skipping of exon 3 alone (Fig. 6D). For FMO5, skipping of exon 3 alone was detected in human kidney and liver (Fig. 6E, lanes 1–3). Skipping of exon 3 in association with skipping of exon 6 and/or 7 was also detected from kidney and liver. In brain, FMO5 transcripts with exon 3 skipped were almost nondetectable (Fig. 6E, lanes 4 and 5).

Characterization of the Catalytic Properties of Exon 3 (Equivalent to Exon 4 for FMO4)-Deleted FMO Proteins. To evaluate the effect of exon 3 (equivalent to exon 4

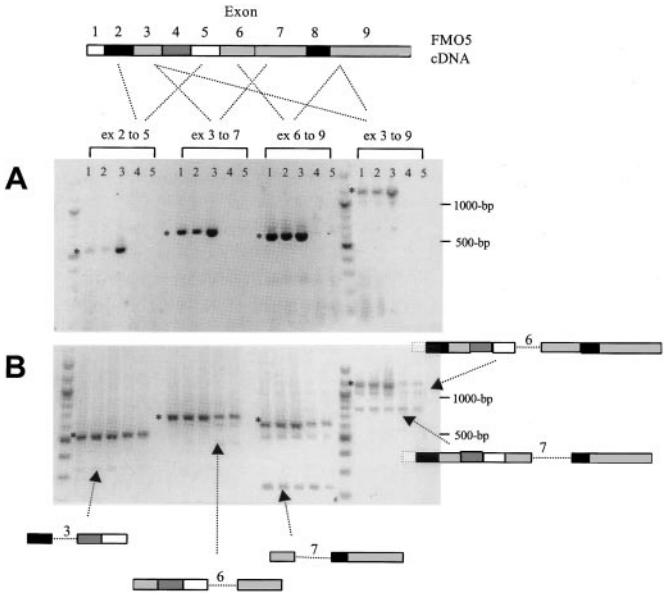

Fig. 5. Alternative processing of the human FMO5 transcript shown by RT-PCR amplification. A diagram of human FMO5 cDNA is shown at the top (each exon is illustrated with different patterned boxes). Specific FMO5 cDNA was synthesized, as described under *Materials and Methods*, from 1 μg of RNA from adult human kidney (lane 1), fetal human liver (lane 2), adult human liver (lane 3), fetal human brain (lane 4), and adult human brain (lane 5). Overlapping fragments (i.e., 2–5, 3–7, 6–9, and 3–9) were amplified with direct PCR (A) or nested PCR (B). The normally spliced transcript is shown with an asterisk. Alternative splice variants are indicated by arrows and illustrated according to the sequence analysis (blocks represent existing exons and dotted lines represent skipping exons).

TABLE 4
Summary of alternative splicing events detected in *FMO1, 2, 3, 4* and *5* based on sequence data of PCR fragments identified in Figure 1–6.

Gene	Skipping of Region	Base Pair Length	Frame Shift
FMO1	Exon 3	189	No
	Part of exon 7	268	Yes
	Exon 8	73	Yes
FMO2	Exon 2	138	Yes
	Exon 4 + 5	306	No
FMO3	Exon 3	189	No
	Exon 7	356	Yes
FMO4	Exon 3 + 4	329	Yes
	Exon 4	189	No
	Exon 4 + 5	352	Yes
	Exon 6 + 7	343	Yes
	Exon 7	200	Yes
	Exon 8	353	Yes
	Exon 8 + 9	423	No
FMO5	Exon 3	189	No
	Exon 3 + 4 + 5	495	No
	Exon 6	200	Yes
	Exon 6 + 7	553	Yes
	Exon 7	353	Yes

for FMO4) deletion (i.e., corresponding to deletion of 63 amino acids, from amino acid 45 to 107 of FMO) on the function of FMO proteins, wild type FMO1-His_6, FMO3-His_6, and FMO4-His_6 and corresponding exon 3 (equivalent to exon 4 for FMO4)-deleted proteins were cloned into vector pMAL-2c. Human FMO5 was not expressed because of the lack of understanding of substrate specificity. These constructs were overexpressed in *E. coli* JM-109 as described above. After amylose-affinity column chromatography, purification of FMO proteins was achieved with a nickel-affinity column, as described under *Materials and Methods*. Purity of FMO proteins was examined by SDS-PAGE analysis (Fig. 7). The migration of the corresponding recombinant proteins was very close to the predicted mass [MBP-FMO1-His_6, 106.8 kDa (lane 1); MBP-FMO1-Δex3-His_6, 99.3kDa (lane 2); MBP-FMO3-His_6, 106.6 kDa (lane 4); MBP-FMO3-Δex3-His_6, 99.1 kDa (lane 5); MBP-FMO4-His_6, 109.8 kDa (lane 7); and MBP-FMO4-Δex4-His_6, 102.1 kDa (lane 8). The identity of each specific band (indicated by an arrow in Fig. 7) was confirmed by Western blot analysis with specific antibodies (data not shown). The purity of the exon-deleted recombinant proteins was significantly less than that of the full-length construct, probably because of proteolytic degradation. This observation was based on Western blot analysis (data not shown). MBP-FMO4-His_6 was also less pure compared with FMO1 and FMO3, and this was apparently associated with its significantly lower level of expression.

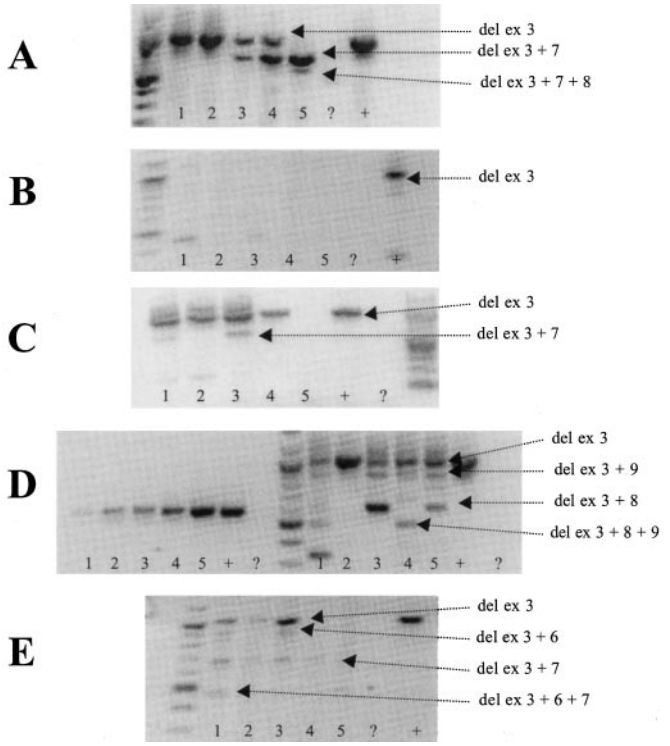

Fig. 6. Alternative splicing of exon 3 (exon 4 for FMO4) in *FMO* genes. Amplification of exon 3-deleted FMO1 (A), FMO2 (B), FMO3 (C), and FMO5 (E) transcripts and exon 4-deleted FMO4 transcripts (D) was done, as described under *Materials and Methods*, from adult human kidney (lane 1), fetal human liver (lane 2), adult human liver (lane 3), fetal human brain (lane 4), and adult human brain (lane 5) samples. Wild-type FMO1, -2, -3, -4, or -5 plasmids and corresponding exon 3 (equivalent to exon 4 for FMO4)-deleted plasmids were used as negative (−) and positive (+) controls, respectively.

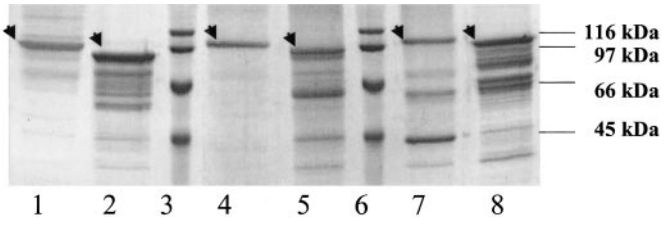

Fig. 7. Analysis of recombinant MBP-FMO-His_6 proteins by SDS-PAGE. MBP-FMO1-His_6 (lane 1), MBP-FMO1-Δex3-His_6 (lane 2), MBP-FMO3-His_6 (lane 4), MBP-FMO3-Δex3-His_6 (lane 5), MBP-FMO4-His_6 (lane 7), and MBP-FMO4-Δex4-His_6 (lane 8) purified protein were fractionated by electrophoresis on polyacrylamide gel in the presence of SDS and stained with Coomassie blue. Lanes 3 and 6 show the position of the molecular mass standards. Arrows point to the bands corresponding to the recombinant proteins.

Methimazole was used to investigate the ability of each variant to catalyze *S*-oxygenation. Methimazole was an excellent substrate for MBP-FMO3-His_6 (i.e., K_m, ~25 μM; V_{max}, ~15 nmol/min/mg) and for MBP-FMO1-His_6 (i.e., K_m, ~40 μM, V_{max}, ~90 nmol/min/mg). No methimazole *S*-oxygenase activity was observed in the presence of MBP-FMO1-Δex3-His_6, MBP-FMO3-Δex3-His_6, MBP-FMO4-His_6, or MBP-FMO4-Δex4-His_6 (detection limit of the assay was 0.2 nmol/min). 5-DPT was used to investigate the ability of each variant to catalyze tertiary amine *N*-oxygenation. 5-DPT-*N*-oxide was detected after incubation of 5-DPT with MBP-FMO3-His_6 or MBP-FMO1-His_6. However, formation of 5-DPT-*N*-oxide was nondetectable after incubation of 5-DPT with MBP-FMO4-His_6 and the corresponding exon 3 (equivalent to exon 4 for FMO4)-deleted FMO1, -3, and -4 proteins (detection limit of the assay was 5 nmol/min).

Discussion

Until recently, it was assumed that proteome complexity in higher eukaryotes was mainly achieved through the differential transcriptional regulation of a large number of genes. The observation that the human genome contains a smaller number of genes than previously predicted increases the chance that alternative splicing makes a contribution to the observed complexity. Because a few splice variants of *FMOs* were described in rabbits (Luo and Hines, 1996; 1997) and rats (Lattard et al., 2003), identification of such events in humans represents an important step to understand the diversity of the FMO family of enzymes. In this report, we systematically analyzed alternative splice variants occurring in *FMO* gene families from different tissues in humans.

To identify the totality of splicing events occurring for each *FMO* gene, a nested PCR amplification strategy was adopted. The size of the amplified fragment was designed to be between 600 and 750 bp to readily detect small size variations of PCR-products. For each FMO, three to four overlapping regions covering the whole coding sequence were amplified. This strategy, followed by the systematic sequencing of the PCR products, allowed the identification of a large number of splice variants in the FMO family. Among the FMO members, the picture of the splicing events observed in *FMO1*, *FMO2*, and *FMO3* were relatively simple: two to three different low-level variants were observed for each gene. In contrast, for *FMO5* and particularly for *FMO4*, the picture was relatively more complex. A large number of splicing events were observed: seven and five different splice variants were identified for *FMO4* (i.e., skipping of exons 3 and 4, 4, 4

and 5, 6 and 7, 7, 8, 8 and 9) and *FMO5* (i.e., skipping of exons 3, 3 and 4 and 5, 6, 6 and 7, 7), respectively. Despite the identification of a large number of FMO splice variants, additional splicing events might exist. In fact, our strategy did not allow the analysis of the presence of the extreme exons (i.e., 1 and 9 or 10 for FMO4). Results from Fig. 6 and preliminary cloning of the total coding sequences for each *FMO* (data not shown) suggest that distinct splicing events can coexist (for example, skipping of exon 3 and skipping of exon 7 in *FMO1*, *-3*, and *-5*). However, this aspect has not yet been fully explored. To better understand how a specific FMO exon was selectively skipped, we evaluated each 5′ donor site and 3′ acceptor sites for each *FMOs* through web-based splice site analysis software (http://www.fruitfly.org/seq_tools/splice.html) (Reese et al., 1997). However, only a few exon skipping events can be associated with weak splicing acceptor sites (i.e., FMO1 exon 3, FMO2 exon 2, FMO4 exon 3, and FMO5 exon 7) and other splicing events cannot be directly associated with these splice sites. In addition, because we used pooled RNA samples during our analysis, it is possible that the measured transcripts represent those derived from a genetically variant individual member of the pooled sample (e.g., a SNP within an exon splicing enhancer). However, most of the splice variants were identified from more than one tissue pool, and the different tissue pools were all from different individuals. This suggests the contribution of a SNP to these splice variants was less likely unless it was caused by very common SNPs.

After the identification of the prominent FMO splice variants, their expression patterns were examined by direct PCR amplifications of the same overlapping regions. The expression patterns of the FMO splice variants identified in this study do not seem to be strongly tissue-specific or specifically associated with fetal or adult tissues. Furthermore, their expression level is generally lower than the expression of the corresponding normally spliced transcript. However, splice variants of FMO4 must be considered separately. Normally spliced FMO4 is expressed in human kidney and liver as the dominant FMO4 species. In contrast, FMO4-splice variants are present at higher levels than "normally spliced" FMO4 in human brain. Detection of FMO4 protein, by Western blot analysis, is difficult in some human tissues (data not shown). This might be a result of the extensive alternative splicing of *FMO4*. The results for FMO4 suggest that regulation of alternative splicing might be a mechanism that is equally important as regulation of the transcription level to control the expression of the corresponding proteins in tissues. In this study, we used pooled human tissue samples to develop a basic understanding of alternative splicing events in *FMO*s. Alternative splicing might result from single nucleotide polymorphisms. To fully explore the regulation of alternative splicing events and its putative association with protein expression, future analysis of individual-, tissue- and age-dependent variations of these different splicing events will be required.

Systematic analysis of multiple PCR-products obtained after nested PCR revealed that a high frequency of alternatively spliced forms of FMOs are present in human tissues. Although *FMO* genes are generally considered to produce single gene products (Lawton et al., 1994), the presence of FMO splice variants suggest that this may not be entirely accurate. Among the identified FMO splice events occurring in humans, the majority of them lead to a frameshift (i.e., skipping of exons 7 and 8 for FMO1; skipping of exon 2 for FMO2; skipping of exon 7 for FMO3, skipping of exons 3 and 4, 4 and 5, 6 and 7, 7, and 8 for FMO4; skipping of exons 6, 6 and 7, and 7 for FMO5). The corresponding transcripts are therefore incapable of encoding a functional enzyme. Other splice events led to the lack of essential functional sites (e.g., NADPH-binding site or FATGY site), rendering any corresponding protein probably nonfunctional (i.e., skipping of exons 4 and 5 for FMO2, skipping of exons 8 and 9 for FMO4, skipping of exons 3 and 4 and 5 for FMO5) (Atta-Asafo-Adjei et al., 1993). In fact, among all the FMO splice variants identified in this study, deletion of exon 3 (equivalent to exon 4 for FMO4) was the most common splice event occurring in FMOs and was readily detectable for *FMO1*, *-3*, *-4*, and *-5*. Study of FMO splicing events showed the existence of transcripts without exon 3 only (exon 4 for FMO4) and transcripts without exon 3 in combination with other deletions in the rest of the coding sequence. Skipping of exon 3 (exon 4 for FMO4) alone is a particularly interesting alternative splicing event. Skipping of this particular exon (i.e., a 189-bp fragment corresponding to 63 amino acids) does not modify the reading frame and might encode new isoforms of FMOs with different catalytic properties. FMO4 transcripts without exon 4 have been previously detected in rat brain (Lattard et al., 2003). The presence of the corresponding protein (i.e., 57 kDa instead of 64 kDa for the full-length protein) was also shown in rat brain (Lattard et al., 2003) by Western blot analysis. In this study, we confirmed the presence of this deleted FMO4 isoform in humans, as well as the presence of exon 3-deleted FMO1, FMO3, and FMO5 isoforms.

There is precedent in the scientific literature that alternative splicing may generate protein isoforms with distinct characteristics (Flouriot et al., 2000; Lazaridis et al., 2000). In this study, in-frame exon-deleted FMO proteins expressed (i.e., MBP-FMO1-Δex3-His_6 and MBP-FMO3-Δex3-His_6) were not able to catalyze the detectable *S*- and *N*-oxygenation of methimazole and 5-DPT, respectively. Despite the presence of the double tags (MBP and His_6), MBP-FMO1-His_6 and MBP-FMO3-His_6 were found to catalyze the oxygenation of both substrates with kinetic parameters comparable with those previously reported for native FMOs (Overby et al., 1997; Kim and Ziegler, 2000). We did not observe detectable catalytic activity for MBP-FMO4-His_6 or MBP-FMO4-Δex4-His_6. Very low yield for the expression of FMO4 fusion proteins was observed, and this was similar to what had been reported previously (Itagaki et al., 1996). Because the full-length FMO4 fusion protein did not show activity in our assays, we could not unambiguously conclude whether or not the exon 4-deleted FMO4 construct was truly inactive. Exon 3 deletion does not seem to preserve the catalytic properties of FMO1 and FMO3 proteins, despite the presence of the cofactor sites (FAD- and NADPH-binding sites) essential for FMO proteins. It is possible that the lack of the 63 amino acids encoded by exon 3 leads to a modification of the protein structure, abolishing the ability of FMO to *S*- or *N*-oxygenate substrates. It is also possible that the catalytic properties of the deleted FMO proteins are significantly modified but nevertheless could recognize and oxygenate other substrates that remain to be discovered.

In summary, in humans, each *FMO* gene produced several transcripts as a result of alternative processing events. Exon

skipping was the major splicing mechanism observed in this study. In only a few cases were splicing events caused by the presence of alternative splicing sites. In contrast to *FMO6* (Hines et al., 2002), some of the splice variants identified for *FMO1, -3*, *-4*, and *-5* can lead to the production of a in-frame exon-deleted protein. For *FMO4,* the observation of many splice variants at significant levels must be considered in any attempt to thoroughly quantify FMO4 transcripts, for which each exon can be skipped.

Acknowledgments

Tissue for this project has been provided in part by the University of Miami Brain and Tissue Bank for Developmental Disorders, in contract to the National Institute for Child Health and Development (NICHD contract NOI-HD-8-3284), by the Brain and Tissue Bank for Developmental Disorders at the University of Maryland at Baltimore, in contract to the NICHD (contract No. NOI-HD-8-3283), and by Stanford Research International (Menlo Park, CA).

References

Atta-Asafo-Adjei E, Lawton MP, and Philpot RM (1993) Cloning, sequencing, distribution and expression in *Escherichia coli* of flavin-containing monooxygenase 1C1. *J Biol Chem* **268:**9681–9689.

Brunelle A, Bi YA, Lin J, Russell B, Lu YC, Berkman CE, and Cashman JR (1997) Characterization of two human flavin-containing monooxygenases (form 3) enzymes expressed in *Escherichia Coli* as maltose binding fusions. *Drug Metab Dispos* **25:**1001–1007.

Cashman JR (1995) Structural and catalytical properties of the mammalian flavin-containing monooxygenase. *Chem Res Toxicol* **8:**165–181.

Christmas P, Jones JP, Patten CJ, Rock DA, Zheng Y, Cheng SM, Weber BM, Carlesso N, Scadden DT, Rettie AE, et al. (2001) Alternative splicing determines the function of CYP4F3 by switching substrate specificity. *J Biol Chem* **276:** 38166–38172.

Dixit A and Roche TE (1984) Spectrophotometric assay of the flavin-containing monooxygenase and changes in its activity in female mouse liver with nutritional and diurnal conditions. *Arch Biochem Biophys* **233:**50–63.

Dolphin CT, Cullingford TE, Shephard EA, Smith RL, and Phillips IR (1996) Differential developmental and tissue-specific regulation of expression of the genes encoding three members of the flavin containing monooxygenase family of man, FMO1, FMO3 and FMO4. *Eur J Biochem* **235:**683–689.

Domanski TL, Finta C, Halpert JR, and Zaphiropoulos PG (2001) cDNA cloning and initial characterization of CYP3A43, a novel human cytochrome P450. *Mol Pharmacol* **59:**386–392.

Flouriot G, Brand H, Denger S, Metivier R, Kos M, Reid G, Sonntag-Buck V, and Gannon F (2000) Identification of a new isoform of the human estrogen receptor-alpha (hER-alpha) that is encoded by distinct transcripts and that is able to repress hER-alpha activation function 1. *EMBO (Eur Mol Biol Organ) J* **19:**4688–4700.

Hines RN, Cashman JR, Philpot RM, Williams DE, and Ziegler DM (1994) The mammalian flavin-containing monooxygenases: molecular characterization and regulation of expression. *Toxicol Appl Pharmacol* **125:**1–6.

Hines RN, Hopp KA, Franco J, Saeian K, and Begun FP (2002) Alternative processing of the human FMO6 gene renders transcripts incapable of encoding a functional flavin-containing monooxygenase. *Mol Pharmacol* **62:**320–325.

Itagaki K, Carver GT, and Philpot RM (1996) Expression and characterization of a modified flavin-containing monooxygenase 4 from humans. *J Biol Chem* **271:** 20102–107.

Kim YM and Ziegler DM (2000) Size limits of thiocarbamides accepted as substrates by human flavin-containing monooxygenase 1. *Drug Metab Dispos* **28:**1003–1006.

Laemmli UK (1970) Cleavage of structural proteins during the assembly of the head of bacteriophage T4. *Nature (Lond)* **227:**680–685.

Lattard V, Longin-Sauvageon C, and Benoit E. (2003) Cloning, sequencing and tissue distribution of rat flavin-containing monooxygenase 4: two different forms are produced by tissue-specific alternative splicing. *Mol Pharmacol* **63:**253–261.

Lawton MP, Cashman JR, Cresteil T, Dolphin CT, Elfarra AA, Hines RN, Hodgson E, Kimura T, Ozols J, Phillips IR, et al (1994) A nomenclature for the mammalian flavin-containing monooxygenase gene family based on amino acid sequence identities. *Arch Biochem Biophys* **308:**254–257.

Lazaridis KN, Tietz P, Wu T, Kip S, Dawson PA, and LaRusso NF (2000) Alternative splicing of the rat sodium/bile acid transporter changes its cellular localization and transport properties. *Proc Natl Acad Sci USA* **97:**11092–11097.

Lomri N, Gu G, and Cashman JR (1992) Molecular cloning of flavin containing monooxygenase (form II) cDNA from adult human liver. *Proc Natl Acad Sci USA* **89:**1685–1689.

Luo Z and Hines RN (1996) Identification of multiple rabbit flavin-containing monooxygenase form 1 (FMO1) gene promoters and observation of tissue-specific DNase I hypersensitive sites. *Arch Biochem Biophys* **336:**251–260.

Luo Z and Hines RN (1997) Further characterization of the major and minor rabbit FMO1 promoters and identification of both positive and negative distal regulatory elements. *Arch Biochem Biophys* **346:**96–104.

McCombie RR, Dolphin CT, Povey S, Phillips IR, and Shephard EA (1996) Localization of human flavin-containing monooxygenase genes *FMO2* and *FMO5* to chromosome 1q. *Genomics* **34:**426–429.

Mironov AA, Fickett JW, and Gelfand MS (1999) Frequent alternative splicing of human genes *Genome Res* **9:**1288–1293.

Overby LH, Carver GC, and Philpot RM (1997) Quantitation and kinetic properties of hepatic microsomal and recombinant flavin-containing monooxygenases 3 and 5 from humans. *Chem Biol Interact* **106:**29–45.

Reese MG, Eeckman FH, Kulp D, and Haussler D (1997) Improved splice site detection in genie. *J Comp Bio* **4:**311–323.

Shephard EA, Dolphin CT, Fox MF, Povey S, Smith R, and Phillips IR (1993) Localization of genes encoding three distinct flavin-containing monooxygenases to human chromosome 1q. *Genomics* **16:**85–89.

Zaphiropoulos PG (1996) Circular RNAs from transcripts of the rat cytochrome P450 2C24 gene: correlation with exon skipping. *Proc Natl Acad Sci USA* **93:**6536–6541.

Ziegler DM (1988) Flavin-containing monooxygenases: catalytic mechanism and substrate specificities. *Drug Metab Rev* **19:**1–32.

Address correspondence to: John R. Cashman; Human BioMolecular Research Institute, 5310 Eastgate Mall, San Diego CA, 92121. E-mail: jcashman@hbri.org